STUDIA UBB CHEMIA, LXI, 4, 2016 (p. 147 - 162)
(RECOMMENDED CITATION)

SYNTHESIS OF MAGNETIC IRON OXIDES FROM FERROUS SULFATE AND SUBSTITUTES AMINES

MARCELA STOIA[a], ANDRA TAMAȘ[a,*], GERLINDE RUSU[a], JEAN MOROȘANU[a]

ABSTRACT. In this paper, magnetic iron oxides were synthesized by using a modified Ueda method starting from ferrous sulfate as iron precursor and different substitued organic amines as precipitants. The evolution of the obtained iron oxides with the annealing temperatures was monitored by thermal analysis, FTIR spectroscopy and X-ray diffractometry. The magnetic powders obtained have been characterized by SEM microscopy and magnetic measurements.

Keywords: *iron oxides, magnetic, substitutes amines, thermal analysis*

INTRODUCTION

Magnetic nanoparticles of iron oxides (e.g Fe_3O_4, γ-Fe_2O_3) have attracted attention in biomedical applications like drug delivery systems, magnetic resonance imaging, and cancer therapy [1-4], but also as adsorbents in water purification due to their numerous advantages [5].

Many synthesis routes were developed for obtaining magnetite: coprecipitation of Fe(II) and Fe(III) hydroxides [6], precipitation of Fe(II) hydroxide and oxidation [7], spray pyrolysis [8], sol-gel [9], thermal decomposition of different precursors [10], combustion [11], hydrothermal [12], solvothermal [13], ball-milling [14] etc. However, magnetite nanoparticles are very much susceptible to air oxidation even at low temperatures [15,16]. The heating of magnetite nanoparticles in air at low temperatures leads to maghemite, while at higher temperatures maghemite is further oxidized to hematite [17]. Maghemite has the same crystalline structure as magnetite, namely spinel ferrite. Bulk magnetite

[a] *University Politehnica Timișoara, Faculty of Industrial Chemistry and Environmental Engineering, 6 Vasile Pârvan str., RO-300223,Timișoara, Romania*
* *Corresponding author: andra.tamas@upt.ro*

and maghemite possess ferrimagnetic properties at room temperature [18]. Many papers about nanostructured iron oxides do not clearly differentiate between both spinel-type iron oxides, since they are very similar. Moreover, particle size and particle size distribution (besides phase composition) are key factors that determine the specific loss power [19].

Due to this susceptibility to oxidation, it is very difficult to synthesize and stabilize pure magnetite; in most cases a mixture of magnetite and maghemite is obtained [20].

There are various coprecipitation routes for the preparation of magnetite nanoparticles, but in most cases synthesis is performed in an inert gas atmosphere, which is bubbling within the solvent to remove dissolved oxygen and to prevent oxidation of Fe(II) into Fe(III) [21]. In this method, Fe^{2+} and Fe^{3+} ions are generally precipitated in alkaline solutions, such as NH_4OH, KOH or NaOH. In most cases, the syntheses are performed at 70-80°C or higher temperatures [22].

Magnetite can be obtained only from Fe^{2+} in the presence of various types of amines: hydroxylamine sulfate [23], bispyridoxylidene hydrazine phthalazine [24], dodecylamine [25]. Only the precipitation of Fe^{2+}, followed by oxidation with H_2O_2 [26,27] or $NaNO_2$ [28] can be also used. Another method uses only Fe^{3+} for precipitation, followed by partially reducing of ferric to ferrous ion by Na_2SO_3 [29] in the precipitation product.

In this paper we report the synthesis of magnetic iron oxides using a modified Ueda method [30,31], starting from ferrous sulfate as iron precursor and different substituted organic amines (diethanolamine, triethanolamine, diethylamine and triethylamine) as precipitants. The evolution of the obtained iron oxides with the annealing temperatures was monitored by thermal analysis, FTIR spectroscopy and X-ray diffractometry. The magnetic powders obtained have been characterized by SEM microscopy and magnetic measurements.

RESULTS AND DISCUSSION

The powders synthesized by ethanolamines have been different from the ones obtained with ethylamines. Firstly, their colour is significantly different: the two powders obtained with ethanolamine (FeDEOA and FeTEOA) had a greenish-brown colour, while the powders obtained with ethylamine (FeDEA and FeTEA) were brown-black. Secondly, the powders FeDEOA and FeTEOA were almost nonmagnetic, while the powders FeDEA and FeTEA had strong magnetic properties. Thus, we concluded that in case of ethanolamines some iron (III) oxyhydroxides are formed, while in case of ethylamines magnetite might be the precipitation product.

All the initial powders have been characterized by TG/DSC thermal analysis in air and in nitrogen, in order to investigate their thermal evolution. The thermal behavior of the powders prepared with ethanolamines (Figure 1) is clearly different from the one of the powders obtained from alkylamines.

Thus, in the case of the samples synthesized with DEOA (Figure 1a) and TEOA (Figure 1b), there are three mass losses. The first mass loss, of about 6% for DEOA and 4% for TEOA, registered in the range 25-150°C, corresponds to the elimination of the adsorbed water, having an endothermic effect associated on DSC with a minimum around 60°C. The main mass loss of about 9% for DEOA and 5% TEOA, that takes place in the range 150-350°C, accompanied by an endothermal effect on DTA curve with minimum about 250°C, suggests a dehydration process of the possible precipitation of FeO(OH) to α-Fe_2O_3. This endothermic effect was reported in literature around 340°C [32] and was evidenced to be dependent on the goethite particle size, concluding that a small-sized goethite, with a high specific surface area, would generally feature a single peak transition, occurring at lower temperatures.

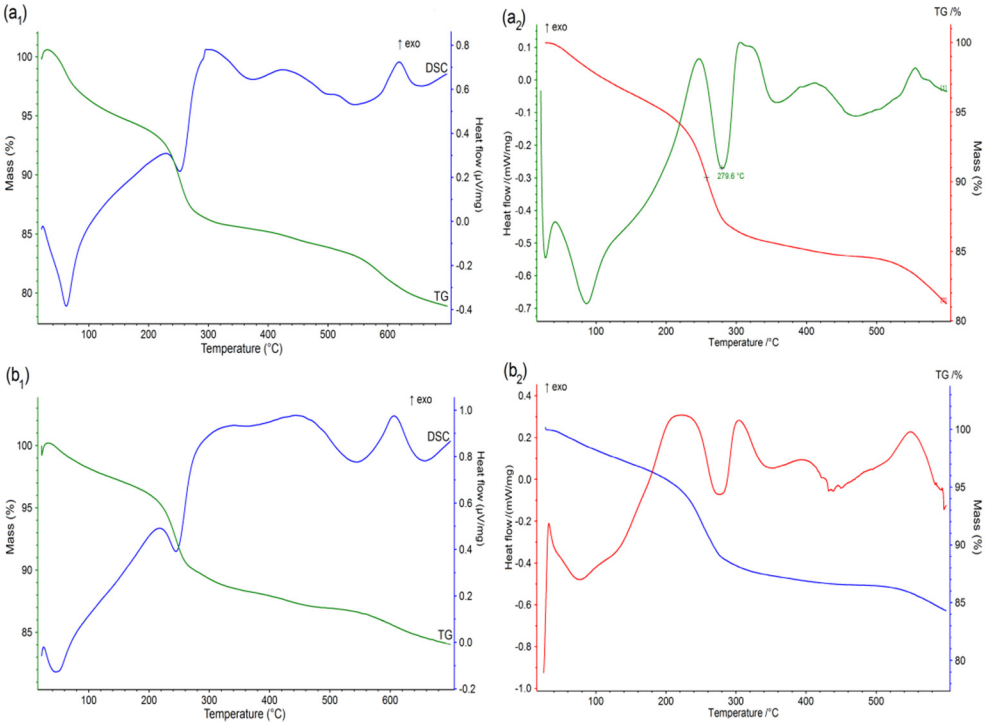

Figure 1. TG/DSC curves of the synthesized powders: (a) FeDEOA and (b) FeTEOA in nitrogen (1) and in air (2) atmosphere;

Comparing the experimental mass losses in this range with the theoretical one (10.1% corresponding to 2FeO(OH) => Fe_2O_3 + H_2O) it results that, in our case, the powders are not formed from pure goethite, but there are probably other iron oxides formed during precipitation. In the range 400-500°C, a weak exothermic effect is registered during a small continuous mass loss. This effect may suggest a crystalline phase transition (possible maghemite to hematite) more visible when using air atmosphere (Figure 1a_2, b_2). The presence of this process in case of heating in nitrogen can only be due to the air contained in the pores of the analyzed powder.

The third small mass loss, correlated with an exothermic effect on DSC curve around 600°C, must be due to a final dehydroxylating step, overlapped with the crystallization of α-Fe_2O_3 from the possible present maghemite that can results by dehydration of lepidocrocite [33].

By comparing the thermal curves registered in nitrogen (Figure 1a_1, b_1) with the ones registered in air (Figure 1a_2, b_2) one can see, that there is a great similarity. The thermal behavior exhibits the same decomposition steps, and the corresponding mass losses did not differ significantly.

In order to confirm the thermal evolution of the powders we have characterized, by FTIR spectroscopy, the powders FeDEOA and FeTEOA as synthesized and annealed at 150°C, 300°C and 450°C, in air, for 3 hours. The obtained FTIR spectra in the range 1200-400 cm^{-1} are shown in Figure 2. The evolution of the two samples is similar. The main difference between the spectra of the as synthesized sample and the one annealed at 150°C, is the significant decrease in intensity of the bands characteristic to the adsorbed water molecules: the large bands in the range 3500-3000 cm^{-1} and 1643 cm^{-1}, confirm the elimination of water in this range of temperature.

The band from the range 3500-4000 cm^{-1} presented two shoulders (two minima) around 3350 cm^{-1} and 3180 cm^{-1}: the shoulder at 3400 cm^{-1} was assigned in literature [34] to the stretching mode of H_2O molecules, whereas the shoulder at 3140 cm^{-1} can be assigned to the stretching mode of the OH group in a goethite structure. In Figure 2, we have illustrated only the range 1200-400 cm^{-1} for a better highlight of the bands characteristic to iron oxides. The bands located around 1130 cm^{-1}, which can be assigned to hydroxyl groups, decrease their intensities by raising the temperature to 150°C, showing that, in the range 25-150°C, a partial dehydroxylating also takes place.

The two central FTIR bands located at 887 cm^{-1} and 794 cm^{-1} can be assigned to Fe-O-H bending vibrations in α-FeOOH, according to Music at al [35]. The broad bands located around 600 cm^{-1} and 450 cm^{-1} were assigned by the same authors to an amorphous iron(III) hydroxyde, or to ferrihydrite. The band located around 600 cm^{-1} increases in intensity, especially in the case of the FeTEOA powder, probably due to the formation of some magnetite by the

thermal decomposition of goethite, as it has been evidenced in literature [36]. The thermal treatment at 300°C leads to significant changes in the FTIR spectra. Thus, the bands characteristic to –OH vibrations from goethite are no longer present, proving the complete dehydration, with the formation of a magnetic phase, probably a mixture of hematite - confirmed by the pronounced bands located at 449 cm^{-1} and ~549 cm^{-1} [37], and maghemite- confirmed by the shoulder located at 630 cm^{-1} [38]. The other bands of maghemite overlapped with hematite bands.

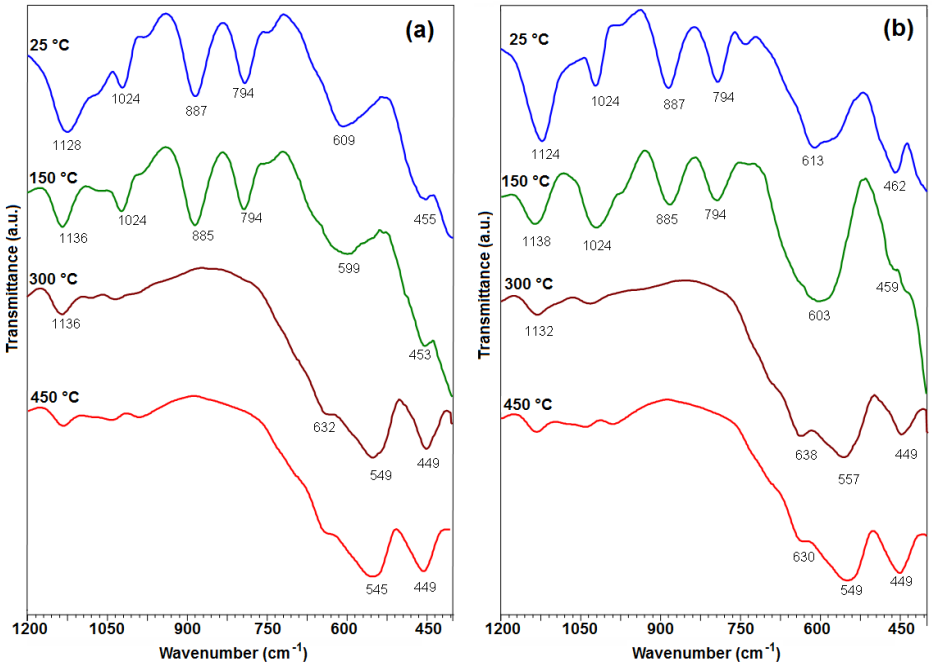

Figure 2. FTIR spectra of the powders FeDEOA (a) and FeTEOA (b) thermally treated

The increase of the annealing temperature at 450°C does not produce significant changes in the FTIR spectra, as also results from thermal behavior. The XRD patterns of the powders FeDEOA and FeTEOA, annealed at different temperatures, are shown in Figure 3 a,b. The evolution of the crystalline phases in the studied samples are similar.

Thus, the powders obtained at room temperature, without thermal treatment, contain a spinel phase, identified as magnetite (JCPDS card no. 01-080-6403) [39], and iron(III) oxyhydroxyde FeO(OH) as two crystalline phases:

goethite (JCPDS card no. 04-015-8332), and lepidocrocite (JCPDS card no. 00-044-1415). The thermal treatment at 150°C does not change the crystalline phase composition of the two powders. After annealing the powders at 300°C, both goethite and lepidocrocite dissapear, as a result of the dehydration evidenced through thermal analysis. According to literature, lepidocrocite (γ-FeOOH) thermally decomposes above 200°C to γ-Fe_2O_3, while goethite (α-FeOOH) decomposes to α-Fe_2O_3 [33]. The main crystalline phase is a spinel phase, identified as γ-Fe_2O_3 (JCPDS card no. 00-039-1346) instead of magnetite, as it is well known that magnetite is oxidized above 200°C, in air, to maghemite [40]. Also, a second low crystalline phase, identified as α-Fe_2O_3 (JCPDS card no. 04-002-7501) is present. One can notice from the XRD patterns of powders annealed at 450°C (Figure 3a,b) that in case of sample FeTEOA the content of hematite is significantly lower compared to FeDEOA, due to its initial lower content of goethite.

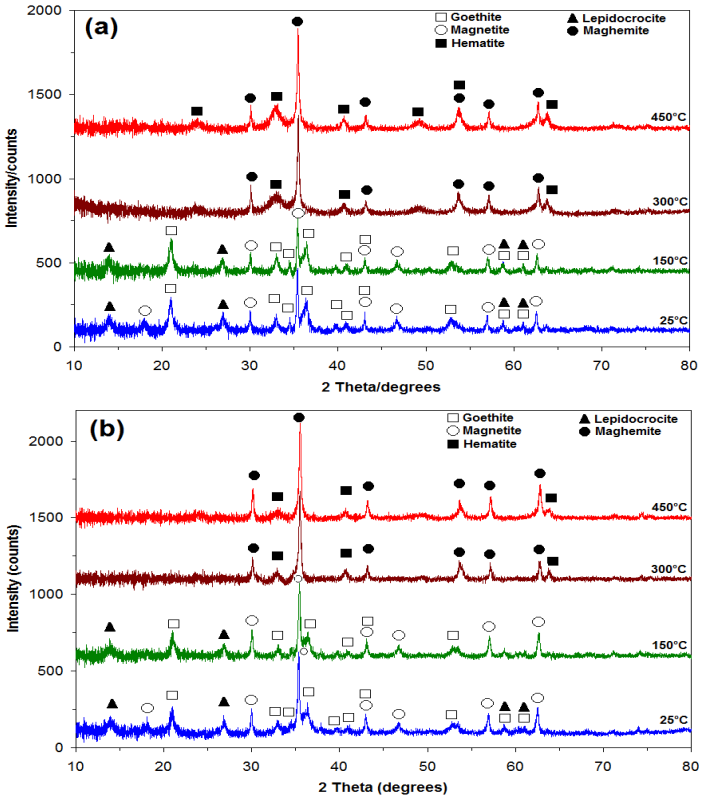

Figure 3. XRD pattern of the powders FeDEOA (a) and FeTEOA (b) thermally treated

We can conclude that in case of the powders synthesized with ethanolamine, the magnetic maghemite phase is stabilized up to 450°C, representing the predominant phase for the powder annealed at this temperature.

The powders FeDEA and FeTEA, as expected, showed a completely different thermal behavior compared to FeDEOA and FeTEOA. Figure 4 shows the TG/DSC curves for the as synthesized powders FeDEA and FeTEA.

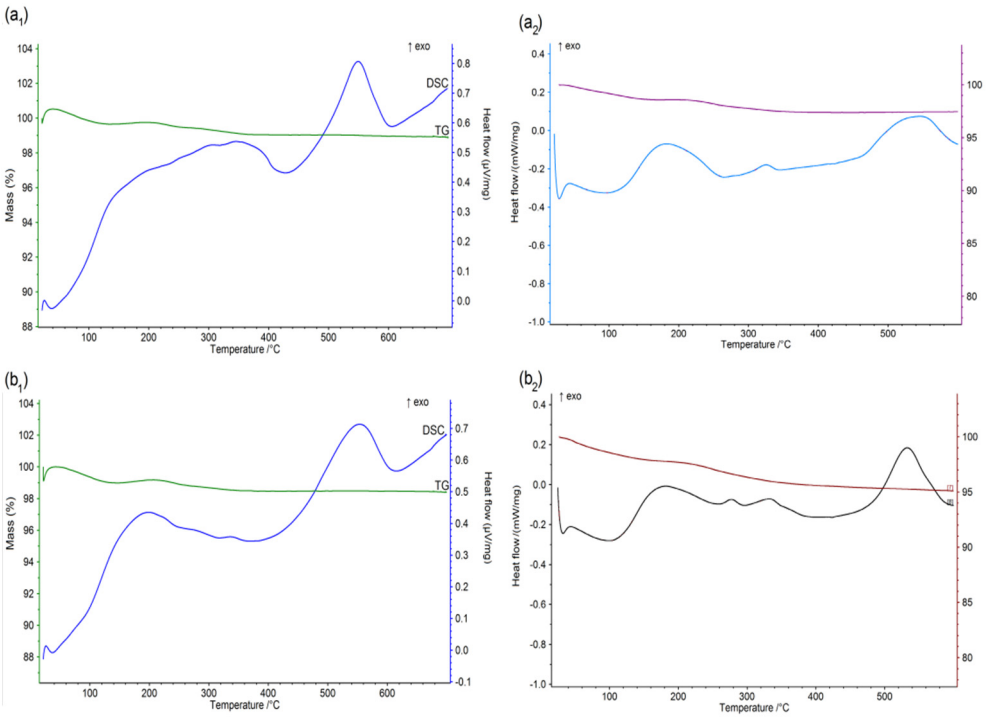

Figure 4. TG/DSC curves of the synthesized powders: (a) FeDEA and (b) FeTEA

One can notice from the TG curves that powder mass does not change significantly during heating up to 600°C, concluding that in this case the desired phase, namely magnetite, was obtained in the as synthesized samples. Even if the heating was performed in nitrogen atmosphere, a slight mass increase is registered in the range 150-220°C, characteristic to magnetite (Fe_3O_4) oxidation at maghemite [41], associated on DSC curve, especially in case of FeDEA (Figure 4a) by an exothermic effect. This can be explained by the presence of air within the powder pores. Above 220°C, the mass no longer changes, but on DSC curve

appears a pronounced exothermic effect with maximum around 550°C, which can be assigned to the transition of maghemite (γ-Fe_2O_3) to hematite (α-Fe_2O_3) [42]. The shape of TG curves in air atmosphere is similar. The mass change is small, but the exothermic effects registered around 200°C are better evidenced, due to the fact that in air, the oxidation process of magnetite to maghemite is more pronounced.

The FTIR spectra of FeDEA and FeTEA powders are shown in Figure 5.

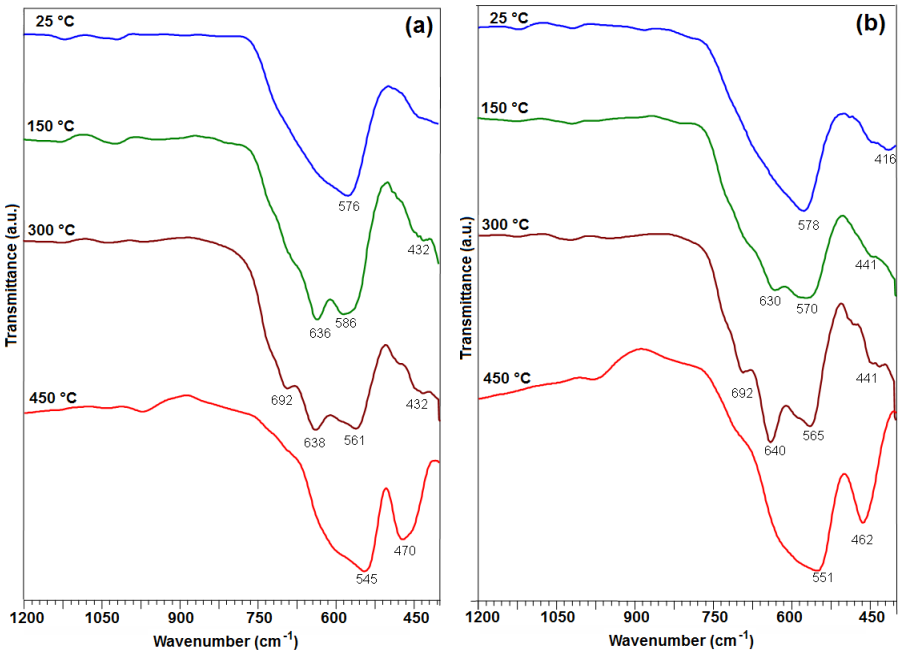

Figure 5. FTIR spectra of the powders FeDEA (a) and FeTEA (b) thermally treated

The single (large) band located in the region 400-600 cm^{-1}, with a maximum at 576cm^{-1} registered in the FT-IR spectra of the as synthesized powders FeDEA and FeTEA, evidenced the formation of magnetite as major phase. The asymetry of the band, suggests the presence of another phase with bands located in this range, most probably maghemite. This hypothesis is confirmed by the splitting of this band after the thermal treatment at 150°C, with appearance of a new band around 630 cm^{-1}, together with the band at 430°C characteristic to maghemite [38]. One can notice that the content of maghemite in the powder FeTEA annealed at 150°C is lower, compared to the powder FeDEA. After being annealed at 300°C, both powders contain only

maghemite, evidenced by the bands located at 692 cm^{-1}, 630 cm^{-1}, 560 cm^{-1}, 430 cm^{-1}. The annealing of these powders to 450°C leads to significant changes in their FTIR spectra. Thus, both spectra (Figure 5 a,b) evidence two strong bands located around 460 cm^{-1} and 550 cm^{-1}, characteristic to α-Fe_2O_3 phase [43]. The width and asymmetry of the band located around 550cm^{-1} may be due to the incomplete transition of maghemite to hematite.

The XRD patterns of powders FeDEA and FeTEA, annealed at different temperatures are shown in Figure 6 a,b.

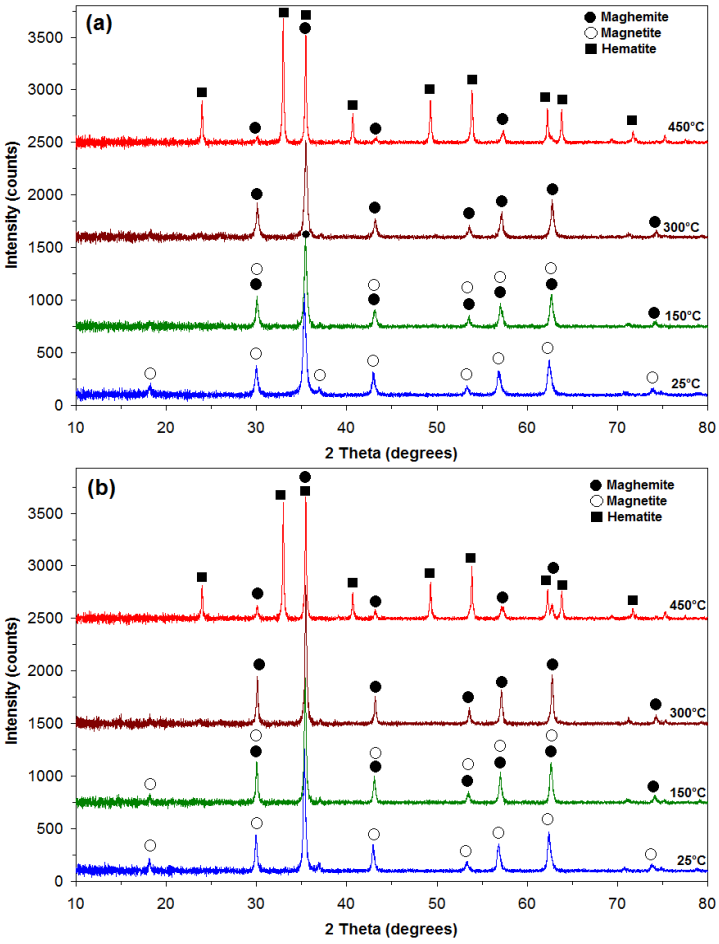

Figure 6. XRD pattern of the powders FeDEOA (a) and FeTEOA (b) thermally treated in air

One can see that the evolution of the crystalline phases with the annealing temperature is similar for the two powders. Starting with the room temperature and up to 300°C as annealing temperature, both powders present a single spinel crystalline phase, with magnetic properties (it gets magnetized under the field of a permanent magnet). This phase was assigned, in case of the as synthesized powders (room temperature) to magnetite (Fe_3O_4) while for the powders annealed at 300°C, it was assigned to maghemite (γ-Fe_2O_3), based on the thermal behavior and FT-IR study. This is in agreement with the literature [18,40]. A detail which sustains our assignment is also the slight but visible shift of the diffraction peaks (especially in case of (511) diffraction peak located around 62 degree) characteristic to the spinel phase to higher 2theta values, as reported before in literature [20]. In case of powders annealed at 150°C, we can consider that we have a mixture of magnetite and maghemite, the position of the diffraction peaks being intermediary between the ones at room temperatures and the ones at 300°C.

The evolution of the crystalline phases can be reflected by the magnetic behavior of the powders. Thus, all the powders obtained at room temperatures and the powders FeTEOA and FeTEA annealed at different temperatures have been characterized by magnetic measurements. The values of the saturation magnetization (M_s), coercive field (H_c) and saturation field (H_s) are listed in the Table 1.

Table 1. The values of magnetic parameters

Sample	Annealing temperature (°C)	M_S (emu g^{-1})	H_c (kA m^{-1})	H_s (kA m^{-1})
FeDEOA	25	8	38	382
FeTEOA	25	20	32	302
	150	20	33	363
	300	27	29	400
	450	18	29	412
FeDEA	25	54	38	383
FeTEA	25	55	37	470
	150	53	38	391
	300	57	35	385
	450	17	37	395

The evolution of the saturation magnetization with the annealing temperature, in case of FeDEA sample, suggests that the powder obtained at room temperature is composed mostly of maghemite, the value of 55 emu g^{-1} being a value characteristic to maghemite nanopowders (up to 60 nm [44]), not to magnetite nanopowders (above 65 emu g^{-1} [45,46]). The insignificant change of the saturation magnetization shows that the composition of the magnetic phase is almost constant up to 300°C. In case of the powder annealed at 450°C, the saturation magnetization suddenly drops, due to the partial transition of magnetic maghemite to nonmagnetic hematite, in agreement with the XRD and FTIR results.

In case of powder FeTEOA the magnetization values of the initial sample and the sample heated at 150°C, are identical due to the constant composition, in agreement with XRD data. The value of the saturation magnetization increases from 20 emu g^{-1} to 27 emu g^{-1} due to the transition of lepidocrocite to magnetic maghemite, while goethite turns into nonmagnetic hematite. The drop of saturation magnetization value to 18 emu g^{-1} after the annealing at 450°C is due to the partial transition of magnetic maghemite to nonmagnetic hematite.

The SEM images of the powders FeTEOA and FeTEA annealed at 150°C and 300°C are shown in Figure 7 and Figure 8.

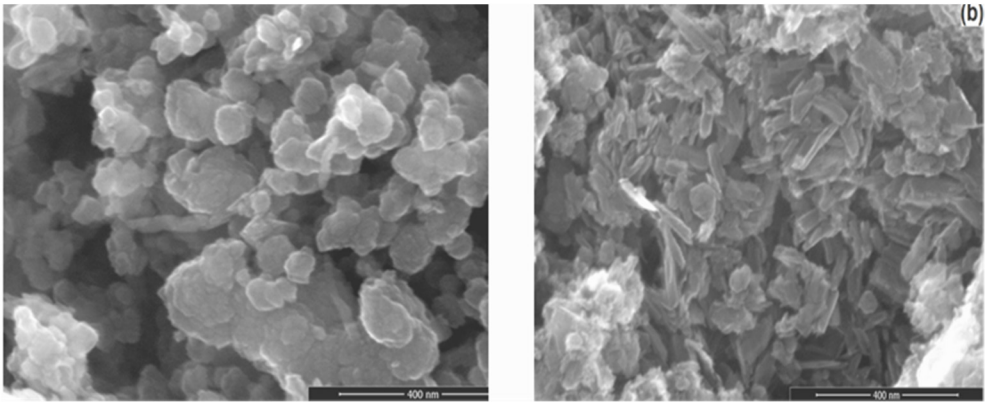

Figure 7. SEM images of powder FeTEOA annealed at 150°C and 300°C

According to the SEM images, both powders are formed from fine quasi-spherical nanoparticles aglomerated in structuress up to hundreds of nanometers, which form micrometrical aggregates. In case of FeTEOA powder, the structures formed by the nanoparticles are less homogenous, and change after the

annealing at 300°C, probably due to the change of crystalline phases. In the case of powder FeTEA, SEM image (Figure 8) evidences ball like structures of nanoparticles, with no significant changes from 150°C to 300°C.

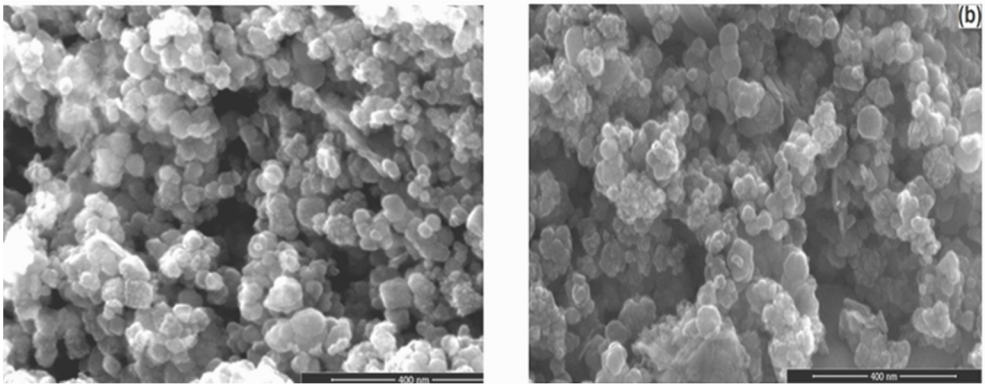

Figure 8. SEM images of powder FeTEA annealed at 150°C and 300°C

CONCLUSIONS

Magnetic iron oxides have been successfully synthesized by a one pot precipitation method starting from iron(II) sulfate and amines in aqueous solutions. TG/DSC simultaneous thermal analysis evidenced the difference in powder composition, the thermal behavior of the powders precipitated with ethanolamines being completely different from that of the powders with ethylamines. Ethanolamines were not able to insure the formation of magnetic iron oxides by precipitation. They led to a mixture of FeOOH and Fe_3O_4, as was evidenced by FTIR, XRD analysis and magnetic measurements. By annealing the obtained powders at 450°C, magnetic maghemite was obtained as the major crystalline phase, impurified with small quantities of hematite. In case of ethylamine, a mixture of magnetite and maghemite was obtained directly from synthesis. After being annealed at 300°C, the powders contain only maghemite. The thermal treatment of these powders at 450°C, led to nonmagnetic hematite as major crystalline phase. The magnetic properties of the powders annealed at different temperature are in agreament with RX results. The saturation magnetization of the powders FeTEOA and FeTEA annealed at 450°C were almost identical, 18 emu g^{-1} and 17 emu g^{-1}, respectively, evidencing the presence of a less crystalline nonmagnetic phase (hematite) in case of FeTEOA powder, and a less crystalline magnetic phase (maghemite) in case of FeTEA powder.

EXPERIMENTAL SECTION

Materials

The starting materials were: ferrous sulfate ($FeSO_4.7H_2O$), diethanolamine-DEOA ($C_4H_{11}O_2N$), triethanolamine-TEOA ($C_6H_{15}O_3N$), diethylamine-DEA ($C_4H_{11}N$), triethylamine-TEA ($C_6H_{15}N$), and sulfuric acid (H_2SO_4) and were all reagent grade, used without further purification.

Synthesis

In a typical synthesis, the quantity of $FeSO_4$ necessary for the synthesis of 0.01 mol of Fe_3O_4 was dissolved in 100 mL distilled water, under addition in drops of H_2SO_4 6M, until complete dissolution, in a 400 mL beaker. The obtained clear solution, was neutralized by addition of the corresponding amine, until the iron hydroxide starts to precipitate. At that moment, the calculated volume of amine (corresponding to an excess of 50% to the stoichiometric quantity necessary for the precipitation of ferrous hydroxide) was quickly added to the ferrous sulfate solution. During the addition of amine, the suspension temperature increases up to 50°C. A viscous, gelatinous precipitate was obtained, which was kept under magnetic stirring for 30 minutes. We have observed that the colours of the precipitates were different. When using DEA and TEA the precipitates were gray, while using DEOA and TEOA they were greenish-black. The beakers have been sealed with a plastic foil and kept in the darkness for 3 days.

Characterization techniques

Thermal behavior of the powders was studied using a NETZSCH STA 449F1 STA449F1A-0220-M, in nitrogen and in air atmosphere, at a flow rate of 20 mL min^{-1}. The TG/DSC curves were recorded in the range of 25-700°C with a heating rate of 10°C min^{-1}, using alumina crucibles. The phase composition of the samples was determined by XRD, using a Rigaku Ultima IV diffractometer ($Cu_{K\alpha}$ radiation). FTIR spectra were carried out using a Shimadzu Prestige-21 spectrometer in the range 400-4000 cm^{-1}, using KBr pellets and a resolution of 4 cm^{-1}. The morphology of the nanopowders was investigated by scanning electron microscopy (SEM), using a FEI Quanta FEG 250 microscope. The magnetic investigation of the final nanopowders was carried out at room temperature, on a Vibrating Sample Magnetometer (DMS VSM).

ACKNOWLEDGMENTS

This work was supported by a grant of the Romanian National Authority for Scientific Research and Innovation, CNCS – UEFISCDI, project number PN-II-RU-TE-2014-4-0514. Magnetic measurements were performed at Research Centre for Complex Fluid Systems Engineering, Politehnica University Timisoara, Mihai Viteazu Street 1, 300222 Timisoara, Romania.

R E F E R E N C E S

[1]. M. Wahajuddin, *International Journal of Nanomedicine,* **2012**, *7*, 3445.
[2]. X. M. Liu, J.K. Kim, *Materials Letters,* **2009**, *63*, 428.
[3]. Y.S. Li, J.S. Church, A.L. Woodhead, F. Moussa, *Spectrochimica Acta Part A*, **2010**, *76,* 484.
[4]. M.D. Shariful Islam, Y. Kusumoto, J. Kurawaki, M.D. Abdulla-al-Mamun, H.A. Manaka, *Bulletin of Materials Science,* **2012**, *35(7)*, 1047.
[5]. X. Jing-San, Z. Ying-Jie, *Journal of Colloid and Interfacial Science*, **2012**, *385*, 58.
[6]. L. Shen, Y. Qiao, Y. Guon, S. Meng, G. Yang, M. Wu, J. Zhao, *Ceramics International,* **2014**, *40*, 1519.
[7]. J.R. Correa, D. Canetti, R. Castillo, J.C. Llopiz, J. Dufou, *Materials Research Bulletin,* **2006**, *41*, 703.
[8]. R. Strobel, S.E. Pratsinis, *Advanced Powder Technology*, **2009**, *20*, 190.
[9]. O.M. Lemine, K. Omri, B. Zhang, L. El Mira, M. Sajieddine, A. Alyamani, M. Bououdina, *Superlattices and Microstructures,* **2012**,*52*, 793.
[10]. S.F. Chin, S.C. Pang, C.H. Tan, *Journal of Materials and Environmental Science,* **2011**, *2(3),* 299.
[11]. R. Ianoș, A. Tăculescu, C. Păcurariu, I. Lazău, *Journal of the American Ceramic Society,* **2012**, *95(7),* 2236.
[12]. C.Y. Hawa, F. Mohamed, C.H. Chia, S. Radiman, S. Zakaria, N. Huang, H. Lim, *Ceramics International,* **2010**, *36*, 1417.
[13]. X. Wang, J. Yu, G. Shi, G. Xu, Z. Zhang, *Journal of Materials Science,* **2014**, *49,* 6029.
[14]. M.M. Can, S. Ozcan, A. Ceylan, T. Firat, *Materials Science and Engineering: B,* **2010**, *172,* 72.
[15]. D. Maity, D.C. Agrawal, *Journal of Magnetism and Magnetic Materials,* **2007**, *308*, 46.
[16]. B.K. Szostko, U. Wykowska, D. Satula, P. Nordblad, *Beilstein Journal of Nanotechnology,* **2015**, *6*, 1385.
[17]. J.P. Sanders, P.K. Gallagher, *Journal of Thermal Analysis and Calorimetry,* **2003**, *72*, 777.

[18]. F. Fajaroh, H. Setyawan, A. Nur, I.W. Lenggoro, *Advanced Powder Technology*, **2013**, *24*, 507.
[19]. J. Murbe, A. Rechtenbach, J. Topfer, *Materials Chemistry and Physics,* **2008**, *110,* 426.
[20]. W. Kim, C.Y. Suh, S.W. Cho, K.M. Roh, H. Kwon, K. Song, I.J. Shon, *Talanta*, **2012**, *94,* 348.
[21]. A. Bandhu, S. Mukherjee, S. Acharya, S. Modak, S.K. Brahma, D. Das, P.K. Chakrabarti, *Solid State Communications,* **2009**, *149*, 1790.
[22]. M.C. Mascolo, Y. Pei, T.A. Ring, *Materials,* **2013**, *6(12),* 5549.
[23]. S. Ardizzone, L. Formaro, Mat. Chem.Phys., **1983**, *8*, 125.
[24]. S. Sarel, S. Avramovic, G. Risarn, E.R. Bauminger, I. Feiner, I. Nowik, R. Williams, N.P. Hughes, *Inorg. Chem.,* **1989**, *28*, 4187.
[25]. D. Hu, Y. Wang, Q. Song, *Particuology*, **2009**, *7*, 363.
[26]. Y. Mizukoshi, T. Shuto, N. Masahashi, S. Tanabe, *Ultrasonics Sonochemistry,* **2009**, *16*, 525.
[27]. M. Aslam, E.A. Schultz, T. Sun, T. Meade, V.P. Dravid, *Crystal Growth & Design*, **2007**, *7(3),* 471.
[28]. I. Nedkov, T. Merodiiska, L. Slavov, R.E. Vandenberghe, Y. Kusano, J. Takada, *Journal of Magnetism and Magnetic Materials,* **2006**, *300*, 358.
[29]. S. Qu, H. Yang, D. Ren, S. Kan, G. Zou, D. Li, M. Li, *Journal of Colloid and Interface Science,* **1999**, *215*, 190.
[30]. M. Ueda, S. Shimada, M. Inaga, *Journal of the European Ceramic Society,* **1996**, *16,* 685.
[31]. M.A. Legodi, D. Waal de, *Dyes and Pigments*, **2007**, *74*, 161.
[32]. S. Gialanella, F. Girardi, G. Ischia, I. Lonardelli, M. Mattarelli, M. Montagna, *Journal of Thermal Analysis and Calorimetry,* **2010**, *102(3),* 867.
[33]. V. Balek, J. Subrt, *Pure and Applied Chemistry,* **1995**, *67(11),* 1839.
[34]. M. Gotic, S. Music, S. Popovic, L. Sekovanic, *Croatica Chemica Acta,* **2008**, *81(4),* 569.
[35]. M. Zic, M. Ristic, S. Music, *Journal of Molecular Structure,* **2007**, *834-836,* 141.
[36]. O. Ozdemir, D.J. Dunlop, *Earth and Planetary Science Letters,* **2000**, *177,* 59.
[37]. Y. Wang, A. Muramatsu, T. Sugimoto, *Colloids and Surfaces A: Physicochemical and Engineering Aspects,* **1998**, *134(3),* 281.
[38]. A. Ercuta, M. Chirita, *Journal of Crystal Growth,* **2013**, *380,* 182.
[39]. ***, The Powder Diffraction File (PDF 4+) JCPDS – Joint Committee on Powder Diffraction Standards, ICC – International Center for Diffraction Data, **2012**.
[40]. J.P. Sanders, P.K. Gallagher, *Thermochimica Acta,* **2003**, *406*, 241.
[41]. R. Nayak, J.R. Rao, *Journal of Scientific and Industrial Research,* **2005**, *64*, 35.
[42]. S. Buathong, D. Ung, T.J. Daou, C. Ulhaq-Bouillet, G. Pourroy, D. Guillon, L. Ivanova, I. Bernhardt, S. Begin-Colin, B. Donnio, *The Journal of Physical Chemistry C,* **2009**, *113*, 12201.
[43]. Y.S. Li, J.S. Church, A.L. Woodhead, *Journal of Magnetism and Magnetic Materials,* **2012**, *324,* 1543.

[44]. J.A.R. Guivar, A.I. Martinez, A.O. Anaya, L. De Los Santos Valladares, L.L. Felix, A.B. Dominguez, *Advances in Nanoparticles,* **2014**, *3,* 114.
[45]. D. Maity, S.N. Kale, R. Kaul-Ghanekar, J-M. Xue, J. Ding, *Journal of Magnetism and Magnetic Materials,* **2009**, *321,* 2093.
[46]. T. Hosono, H. Takahashi, A. Fujita, R.J. Joseyphus, K. Tohji, B. Jeyadevan, *Journal of Magnetism and Magnetic Materials,* **2009**, *321,* 3019.